

Article

Kinetic Characterization of a Panel of High-Affinity Monoclonal Antibodies Targeting Ricin and Recombinant Re-Formatting for Biosensor Applications

Michelle Cummins ^{1,3}, Con Dogovski ^{2,4}, Remy Robert ^{1,5}, Malcolm Alderton ², Damien Chong ², David Proll ², Luisa Pontes-Braz ¹, Anna Raicevic ¹, Meghan Hattarki ¹, Stewart Nuttall ¹ and Olan Dolezal ^{1,*}

¹ CSIRO Materials Science and Engineering, Parkville, Victoria 3052, Australia

² Defense Science and Technology Organization, Fishermans Bend, Victoria 3207, Australia

³ The School of Medicine, Deakin University, Waurn Ponds, Victoria 3216, Australia

⁴ Bio21 Institute, The University of Melbourne, Parkville, Victoria 3052, Australia

⁵ The Department of Immunology, Monash University, Clayton, Victoria 3800, Australia

* Author to whom correspondence should be addressed, E-Mail: Olan.Dolezal@csiro.au; Tel.: +613-9662-7229.

Received: 19 February 2014; in revised form: 10 April 2014 / Accepted: 28 April 2014 /

Published: 9 May 2014

Abstract: Ricin is a potent glycoprotein toxin that is structurally composed of two subunits joined via a disulfide bond: a ~30 kDa subunit A (RTA) and a ~32 kDa subunit B (RTB). There are fears of ricin being used as a weapon for warfare and terrorism and, as such, there is an increasing need for the development of immunodiagnostic reagents targeted towards this toxin. This article describes the production and characterization of a panel of six ricin-specific monoclonal IgG antibodies (mAbs), previously selected based upon their ability to inhibit ricin-mediated killing of cultured cells. Subsequent epitope binding analysis using the surface plasmon resonance (SPR) array biosensor (ProteOn XPR36) indicated three distinct, non-competitive binding epitopes (“bins”). The association (k_a) and dissociation (k_d) rate constants and binding affinities (K_D) of each of the mAbs to ricin were also determined by SPR using Biacore T100 instrument. Affinities (K_D) ranged from 0.1 nM to 9 nM. We present the coding sequences of the variable domains of the six mAbs, the expression, kinetic and cytotoxicity assays for two recombinant Fab (rFab) fragments and demonstrate a rFab affinity improvement by chain-shuffling. Together, these antibodies and constituent rFabs represent a panel of reagents for high-affinity recognition of ricin with potential national security biosensor applications.

Keywords: monoclonal antibody; ricin; Fab fragment; SPR; epitope binning

1. Introduction

Ricin toxin (RT) is a glycoprotein, produced by the castor bean plant *Ricinus communis*, which since its discovery in the 1880s has been extensively studied in both medical and basic research [1,2]. With a mouse LD₅₀ of 10–18 µg/kg it represents a highly toxic compound that can be readily extracted from castor oil plant seeds [2]. Structurally, the toxin is composed of a ~30 kDa A subunit (RTA) and a ~32 kDa B subunit (RTB) that are covalently linked via an intermolecular disulfide bond [3]. The A subunit is an RNA N-glycosidase that functions to inactivate eukaryotic ribosomes. The B subunit binds to glycoproteins and glycolipids containing β(1-3)-linked galactose of N-acetylglactosamine residues [4] and mediates attachment of RT to the surface of eukaryotic cells [5]. Once bound, RT is internalized by endocytosis and is trafficked to the endoplasmic reticulum (ER) by vesicular retrograde transport [6,7]. The RTA-RTB heterodimer itself is not active [8], however, upon entering the ER, the disulphide bond which tethers the two subunits is reduced and liberates the enzymatically active form of the A subunit. The A subunit is then transported across the ER membrane into the cytosol where it selectively depurinates a highly conserved adenine residue in the sarcin/ricin loop of 28S rRNA. This results in inactivation of cellular ribosomes, arrest of protein synthesis [9,10] and causes cell death.

Ricin is considered a significant threat in western countries as there is a real potential for the toxin to be used as a weapon for biowarfare and terrorism [11]. This has raised considerable unease in the biosecurity community and consequently the United States Government's Centres for Disease Control and Prevention (CDC) categorizes ricin as a class B toxin whilst the Australian Government's Department of Health and Ageing classifies ricin as a Tier 1 Security Sensitive Biological Agent (SSBA). Most concern lies with the ease with which ricin can be isolated from castor beans, its inherent stability, potency and the lack of treatment options for intoxicated individuals [12,13]. Efforts to counter this threat have focused on the development of potential vaccines and neutralizing antibodies. These included the recombinant derivative of RTA RiVax [13,14], the GD12 monoclonal antibody [15], the combinatorial use of three monoclonal antibodies (RB34, RB37 and RA36) [16] and the more recent development of a humanized neutralizing anti-ricin antibody hD9 [17]. Beyond vaccination, there is also a requirement for the development of ricin detection reagents for use in national security applications and possibly for rapid treatment of ricin intoxication. Antibody-based systems remain the "gold standard" amongst detection technologies [18]. Such platforms are generally robust, reliable, display high-specificity and high sensitivity. These systems may also incorporate smaller antibody-derived fragments, such as Fab fragments, that retain the targeting specificity of whole mAbs, whilst having the added advantage of possessing improved size:binding ratios and lower production costs [19]. Pelat *et al.* [20] has reported on the generation and characterization of phage library-derived human single-chain Fv (scFv) fragments with the capacity to neutralize biological activity of ricin. Similarly Anderson *et al.* [21,22] and Walper *et al.* [23] have generated and characterized phage-library derived single-domain antibodies (sdAbs) against RTA and RTB.

Dertzbaugh *et al.* [24] and Tran *et al.* [25] have described the generation and properties of a panel of monoclonal antibodies with affinity to ricin. The antibodies were selected on their ability to bind ricin in ELISA-based bioassays and/or inhibition of ricin-mediated eukaryotic cell cytotoxicity *in vitro*. In this study, we have further characterized a subset of these mAbs. Specifically, we have performed epitope binning experiments and determined binding rate and affinity constants. In addition, we have cloned and expressed recombinant Fabs for some of these mAbs, thus allowing for sequence-based comparison of antigen-binding paratopes and the development of a suite of reagents for incorporation into biosensor and other advanced assays.

2. Results and Discussion

2.1. Production and Characterization of a Panel of Six Anti-Ricin mAbs

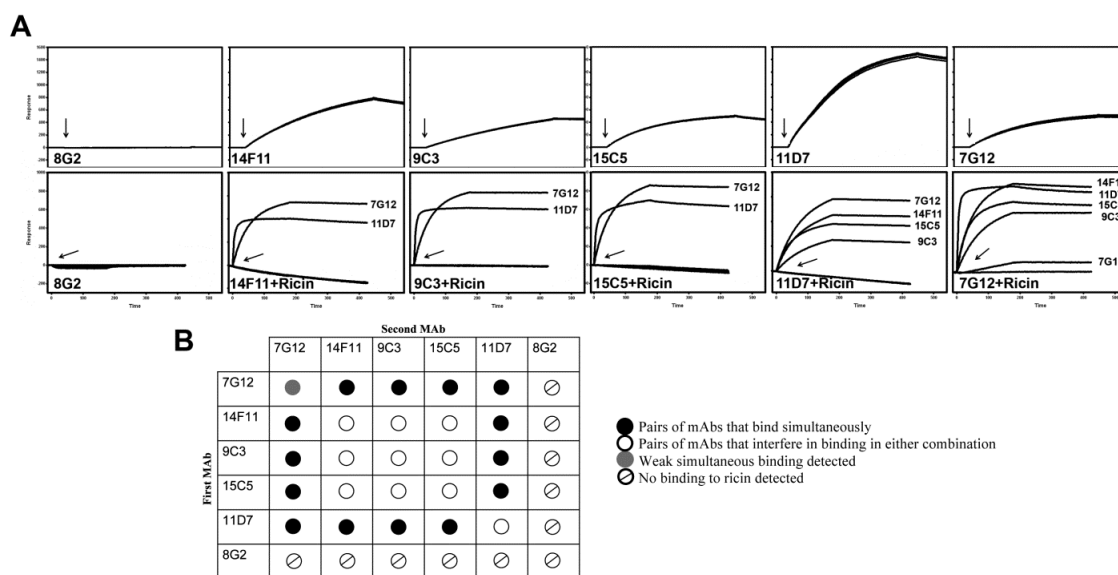
From a panel of previously described mAbs targeting ricin, six mAbs (9C3, 11D7, 14F11, 15C5, 7G12 and 8G2) were selected on the basis of preliminary epitope mapping data [24,25]. In particular, we aimed to analyze these antibodies in terms of their biophysical properties and their suitability as detection reagents. To provide sufficient quantities of reagents for biosensor testing and down-stream characterization, scale-up production of the six mAbs from the serum-free medium was performed. Affinity chromatography on protein A and size exclusion chromatography was utilized for the subsequent purification from serum-free cultures (data not shown).

2.2. Epitope Binding Analysis of mAbs

The specificities and binding characteristics of the purified mAbs were examined using surface plasmon resonance (SPR) measurements. Initially, the ProteOn XPR36 SPR instrument was utilized for epitope binning experiments. Taking advantage of ProteOn's multiplexing capability, a 6×6 antibody-ricin sandwich assay was performed simultaneously. Thus, all six mAbs were immobilized on a GLC chip in the vertical direction. After binding of ricin to this panel (Figure 1A, top panels), the same set of mAbs was injected across the 6 channels in the horizontal direction and binding profiles examined (Figure 1A, bottom panels). For this experimental setup, which is analogous to a sandwich ELISA where the immobilized and injected mAbs are identical, no binding was expected as the ricin epitope for this mAb is already occupied. For example, of the mAbs screened with 14F11 as the primary (immobilized) antibody, only 11D7 and 7G12 still bound ricin, indicating distinct epitopes. Conversely, when the first antibody captured was 11D7 all subsequent mAbs (except 8G2) retained the ability to recognize the bound ricin. An interesting result observed during these experiments was a weak binding signal obtained when 7G12 mAb was passed over 7G12-ricin complex (Figure 1A, bottom right panel). Control injection experiment where 7G12 mAb was shown not to bind to itself or to the chip surface (data not shown) further suggested that 7G12 mAbs may, in fact, recognize a second epitope on ricin surface, albeit with a weak affinity. Unlike for other five mAbs, ricin did not bind to immobilized 8G2 (Figure 1A, top left panel) suggesting that immobilization of 8G2 mAb onto the chip surface destroyed its binding capacity. However, no binding of 8G2 mAb was also observed when ricin was captured via other five mAbs (Figure 1A, bottom panels). Western blot analysis and ELISA with ricin coated to solid support, however, showed that 8G2 mAb bound to ricin and RTA

(data not shown). Although not easily explicable, our findings were consistent with those of Dertzbaugh *et al.* [24] who showed that 8G2 IgG did not bind ricin in ELISA capture format, but bound to ricin on immunoblots or when directly coated to a solid support. These results indicated that the 8G2 may not recognize native form of ricin that is required for SPR assays. Furthermore, it is not unusual that selection of monoclonal antibody clones using plastic-adsorbed antigens (in ELISA wells) can result in selection of mAbs against denatured forms [26]. Using this approach, three distinct bins were detected on ricin with 15C5, 9C3 and 14F11 mAbs belonging to one such bin while 11D7 and 7G12 belonged to two separate bins (Figure 1B). Epitope binning analysis also allowed us to assess the capacity of these mAbs to be used both as a capture reagent when bound to the solid phase and as a detection reagent after the antigen was captured.

Figure 1. Summary of epitope-binning analysis of ricin mAbs using ProteOn XPR36 instrument. (A) Ricin solution (50 nM) was injected (injection points are indicated with arrows) over immobilized mAbs (upper panels). All six mAbs (100 nM) were then injected over mAb+ricin complex (lower panels, mAb injection points are indicated with arrows) and their binding to captured ricin was assessed; (B) The reactivity pattern matrix obtained in binning analysis. At least three distinct epitopes were observed. Monoclonal antibodies 7G12 and 11D7 bind two separate distinct epitopes whilst the third epitope is defined by mAbs 9C3, 14F11 and 15C5. 8G2 did not bind ricin in either orientation.



2.3. Kinetic Analysis of mAbs

To more precisely dissect the kinetics of the mAb-ricin interactions, kinetic analysis was performed using a Biacore T100. Similar to results achieved with the ProteOn XPR36 instrument, no binding of ricin to 8G2 was detected, while the other five mAbs all bound ricin (Figure 2). The association (k_a) and dissociation (k_d) rate constants and the corresponding equilibrium dissociation constants (K_D) determined for the mAbs interacting with whole toxin (RT), ricin subunit B (RTB) and ricin subunit A (RTA) are presented in Table 1. Affinities (K_D) for ricin ranged from 0.15 nM to 8.9 nM (7G12 > 9C3 and 11D7 > 15C5 > 14F11) placing these antibodies in the desired high-affinity bracket for

biological and sensor applications. These SPR results further confirmed preliminary binning results of Dertzbaugh *et al.* [24] which indicated that four of these mAbs (9C3, 11D7, 15C5 and 14F11) bind to RTB whilst 7G12 binds to RTA. Interestingly, 7G12 mAb also showed minor yet reproducible binding interaction with RTB (Figure 2, bottom right panel). Taken together with the results obtained in epitope binning experiments (Figure 1A, bottom right panel) it is possible that this minor interaction occurs as a result of lectin part of ricin (B-chain) interacting with mAb associated glycans. To evaluate this speculation, additional SPR measurements of mAb-ricin interactions with galactose supplemented in the SPR binding buffer as a blocking agent would have to be carried out.

Figure 2. Binding kinetics for ricin interacting with captured mAbs on the chip surface, ricin = RT (left panels), ricin subunit A = RTA (middle panels) and ricin subunit B = RTB (right panels). (A) 14F11; (B) 9C3 (C) 11D7; (D) 15C5 and (E) 7G12. The analytes were injected over captured mAbs at a flow rate of 30 $\mu\text{L}/\text{min}$ for 240-s (RT) or 300-s (RTA and RTB). Data sets that gave a significant dose response were globally fit to a simple 1:1 binding model to obtain the kinetic parameters of the interaction. The black traces represent the experimental data whilst the orange traces represent the fit of a simple 1:1 interaction model to the data.

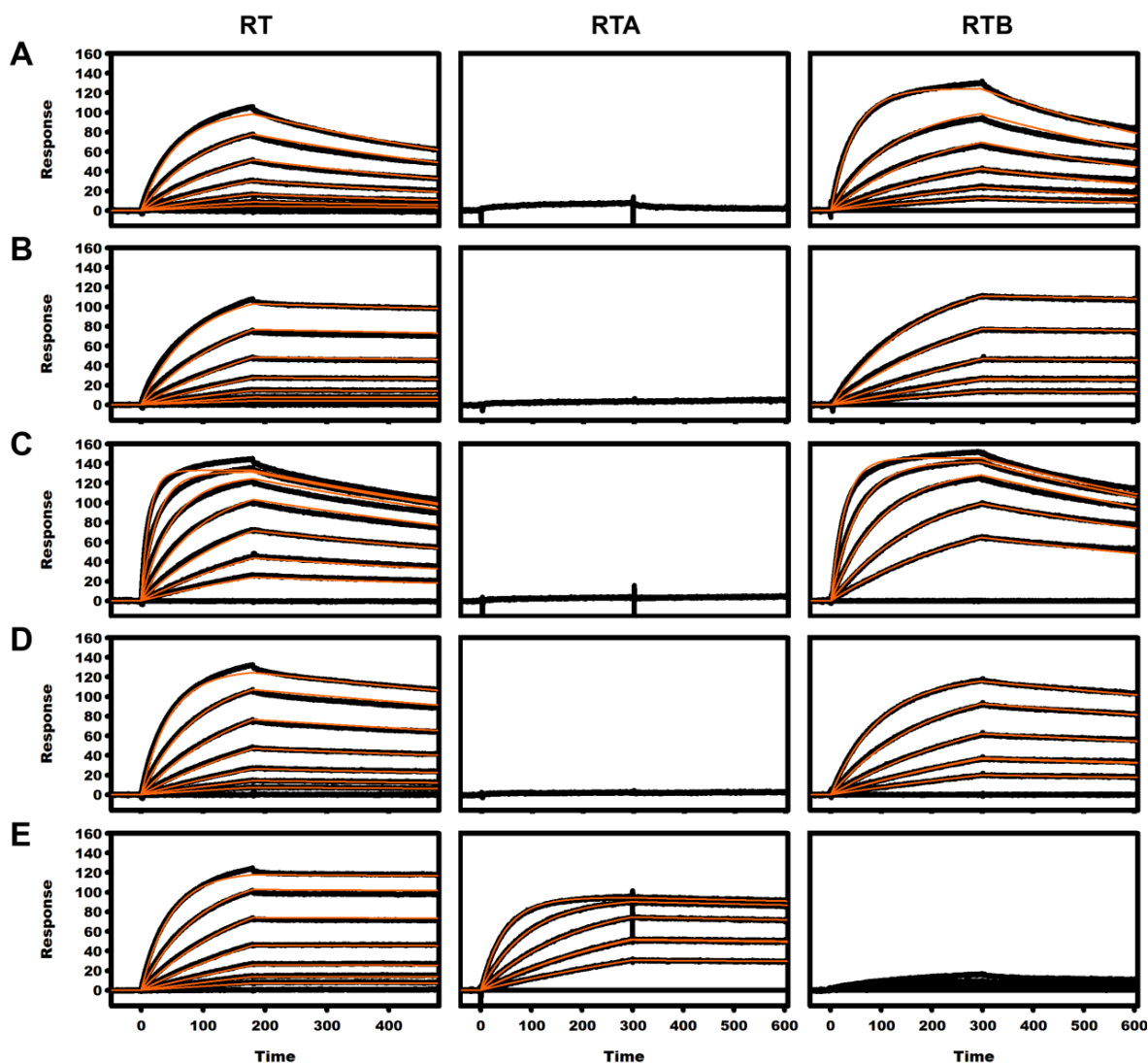


Table 1. Association and dissociation rate and equilibrium dissociation constants of mAbs interacting with ricin (RT: *n* = 3), subunit A (RTA: *n* = 2) and subunit B (RTB: *n* = 2).

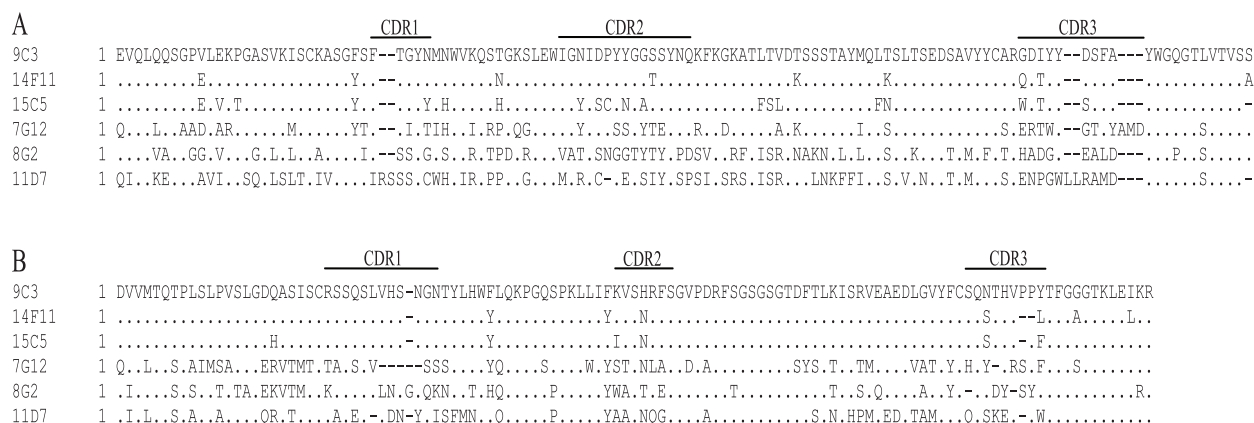
mAb	Analyte	$k_a \times 10^4 (M^{-1} s^{-1})$	$k_d \times 10^{-4} (s^{-1})$	$K_D (nM)$
7G12	RT	21.2 ± 0.3	0.30 ± 0.17	0.15 ± 0.08
	RTA	64.7 ± 6.6	1.1 ± 0.5	0.13 ± 0.2
9C3	RT	11.7 ± 0.5	1.5 ± 0.1	1.3 ± 0.2
	RTB	14.0 ± 0.5	1.3 ± 0.4	0.9 ± 0.3
11D7	RT	74.0 ± 1.8	9.5 ± 0.4	1.3 ± 0.1
	RTB	94 ± 16	9.2 ± 0.2	1.0 ± 0.2
14F11	RT	16.5 ± 0.6	14.5 ± 0.9	8.9 ± 0.9
	RTB	18.0 ± 1.3	11.0 ± 2.2	6.0 ± 0.7
15C5	RT	21.3 ± 0.9	5.0 ± 0.3	2.4 ± 0.2
	RTB	24.0 ± 2.8	4.0 ± 0.1	1.7 ± 0.1
8G2	RT/RTA	NBD	NBD	NBD

NBD = no binding detected.

2.4. Recombinant Fab Antibody Engineering

The next step in obtaining a suite of reagents for biosensor applications was conversion of mAbs to a recombinant format. As an initial step, the antibody V_H and V_L domains were cloned and sequenced from hybridoma (parental) cell lines. Deduced amino acid sequences were consistent with experimentally determined N-terminal residues (data not shown), validating the identity of the antibody genes cloned. High sequence similarity (>90%) in both heavy and light chains was seen for mAbs 9C3, 14F11 and 15C5, but less than 67% similarity for the heavy and light chains of 11D7, 7G12 and 8G2 (Figure 3). This further supported our interpretation of our epitope binning results which suggested that 9C3, 14F11 and 15C5 recognize the same epitope.

Figure 3. Sequence alignment of the mAb heavy and light chains. Alignment of heavy (A) and light (B) chain amino acid sequences using the Global-Reference alignment tool in Clone Manager 9. Like amino acids are represented by (.), gaps introduced into sequences to optimize alignment are represented by (-). CDR regions are labeled according to Kabat’s nomenclature.



Recombinant Fab fragments for 9C3, 11D7, 14F11, 15C5, 7G12 and 8G2 were assembled, and expressed in *E. coli* (Figure 4). Poor bacterial expression was observed for 11D7, 15C5 and 7G12 rFabs and consequently these three constructs were not characterized any further. Recombinant Fab proteins 8G2 (8G2 rFab), 9C3 (9C3 rFab) and 14F11 (14F11 rFab) were purified to homogeneity using a combination of Ni²⁺/NTA affinity and size exclusion chromatography. The final yield of purified 8G2 rFab and 14F11 rFab was approximately 5 times (0.5 mg per liter of bacterial culture) higher than that of 9C3 rFab (0.1 mg/L). SPR binding analysis of all three rFabs was performed using Biacore T100 kinetic experiments with ricin immobilized on the chip surface. As was the case with the parental mAb, no binding to ricin was observed for 8G2 rFab (data not shown). Importantly, 14F11 and 9C3 rFab bound to ricin with similar binding profiles and affinity as their parental mAbs (Figure 5, Table 2). As established in the previous section, 14F11 and 9C3 mAbs bound to the same epitope, an unsurprising result given the high homology between the heavy and light chain sequences (92% and 93% respectively, Figure 3).

Figure 4. Construction of the anti-ricin rFab in pGC (cloning cassette). Variable genes (V_H and V_L) were cloned into the pGC/huchc1 vector preceded by a 5' end *pelB* and *OmpA* signal sequences, respectively. A histidine tag and double FLAG tag sequences are 3' of the $V_H C_{H1}$ and $V_L C_L$, respectively.

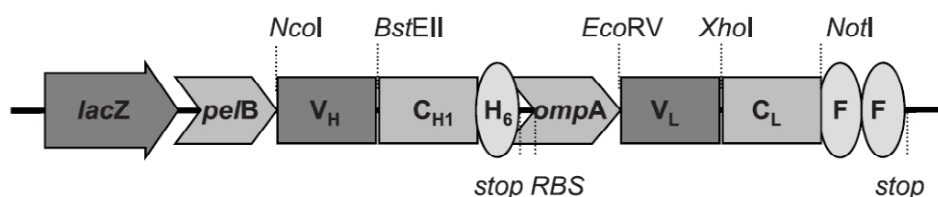


Figure 5. Classical kinetics of rFabs, (A) 14F11; (B) 9C3 and (C) chained-shuffled construct, binding to immobilized ricin. Recombinant Fabs, (concentrations of 0, 0.5 nM, 2 nM, 8 nM, 32 nM and 128 nM) were sequentially injected for 420-s at a flow rate of 30 μ L/min. In the case of the chained-shuffled construct, 64 nM instead of 128 nM top concentration was used. The dissociation phase of the complex was monitored for 900-s except for the highest concentration of chained-shuffled construct where the dissociation was monitored for 1800-s. The black lines represent triplicate experimental data and the orange lines represent the fit to a simple 1:1 interaction model.

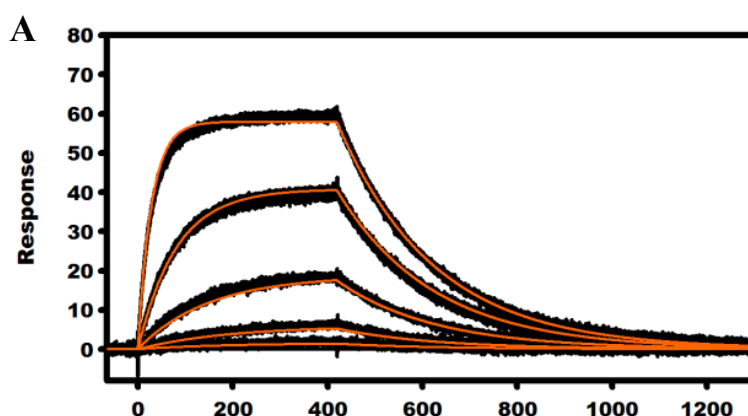
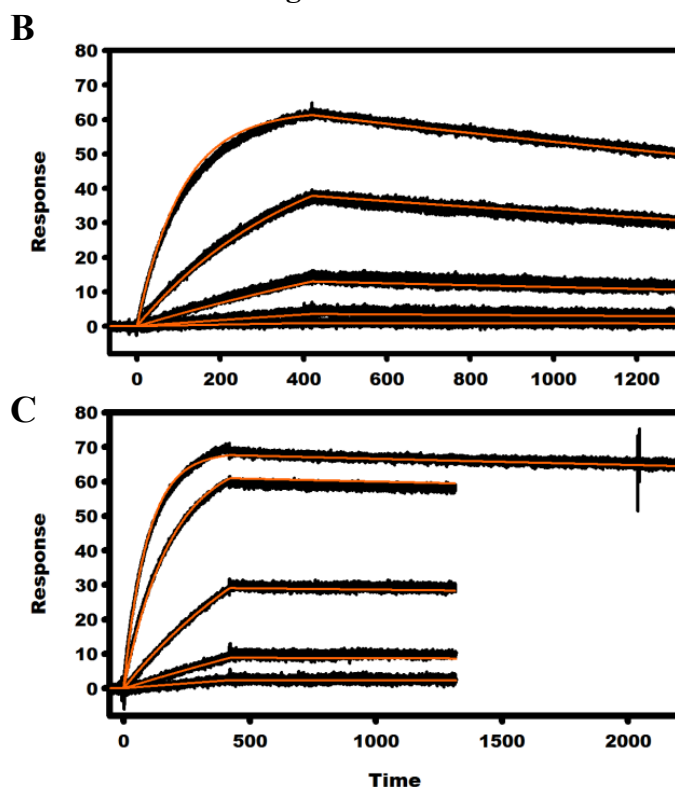


Figure 5. Cont.

**Table 2.** Rate and equilibrium dissociation constants for rFabs binding to ricin ($n = 3$).

rFab	$k_a \times 10^4$ ($M^{-1} s^{-1}$)	$k_d \times 10^{-4}$ (s^{-1})	K_D (nM)
14F11	18.7 ± 0.8	50.0 ± 0.1	27.0 ± 0.6
9C3	9.9 ± 0.5	2.32 ± 0.02	2.3 ± 0.1
Chained-shuffled	23.4 ± 0.5	0.21 ± 0.07	0.13 ± 0.02

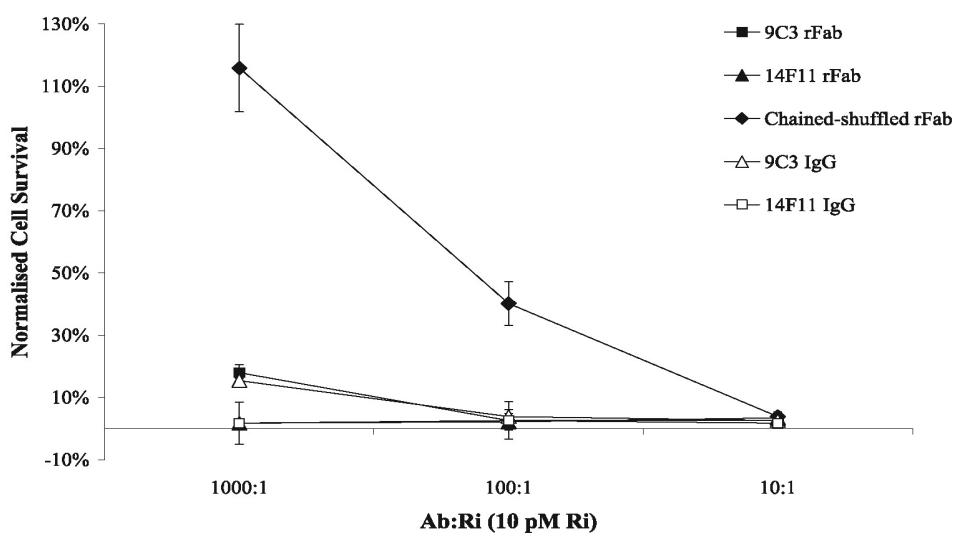
To further engineer anti-ricin rFab fragment for higher affinity, a chain-shuffling strategy was employed whereby the 14F11 rFab light chain was replaced with the 9C3 rFab light chain. The rationale supporting this particular rearrangement was based on two observations: 1) *E. coli* expression levels were higher for the lower affinity construct (14F11), and 2) the difference in affinity between 14F11 and 9C3 could most likely be attributed to the sequence differences within the CDR3 region of the two light chains (Figure 3). Specifically we speculated that the most significant difference likely to affect affinity of the two rFabs was the double-proline insertion within CDR L3 of 9C3. Expression yields for the chained-shuffled rFab (14F11H/9C3L) were equivalent or better when compared with the parental 14F11 rFab. More importantly, when compared with 14F11 and 9C3 rFabs, the affinity of the chained-shuffled rFab to ricin was improved 208- and 18-fold respectively, an enhancement, predominantly due to favorable dissociation kinetics (Table 2, Figure 5).

2.5. Antibody Neutralization of Ricin-Mediated Cytotoxicity Assays

The ability of the three rFab fragments (9C3, 14F11, chain-shuffled) to inhibit ricin-mediated killing of small airway epithelial (SAE) cells *in vitro* was determined and compared with the parental mAbs (Figure 6). The chained-shuffled rFab, showed the greatest protection of the three rFabs tested

and was also superior to the 9C3 mAb which was shown by SPR to have greater than 10-fold weaker affinity (Tables 1 and 2). We attributed this enhanced protection to the better binding kinetics and in particular to the difference in dissociation rate constants. Thus, for example, the estimated k_d in case of the chained-shuffled rFab ($0.21 \times 10^{-4} \text{ s}^{-1}$) was 11-fold and 238-fold lower than in case of 9C3 rFab ($2.32 \times 10^{-4} \text{ s}^{-1}$) and 14F11 rFab ($50 \times 10^{-4} \text{ s}^{-1}$), respectively. Lower k_d values make the antibody-ricin complex more stable and consequently decrease a chance of a ricin molecule detaching from the antibody and penetrating the cell membrane.

Figure 6. Antibody neutralization of ricin-mediated cellular cytotoxicity. Affinity-purified monoclonal antibody (mAb) was mixed with ricin toxin before incubation with small airway epithelial cells in culture. Cytotoxicity was determined using Neutral Red as a vital stain. The Absorbance at 540 nm was determined for each well and used to calculate cytotoxicity relative to an untreated control (% Control). Means were normalized against cells treated with ricin only and expressed as a percentage of the negative control.

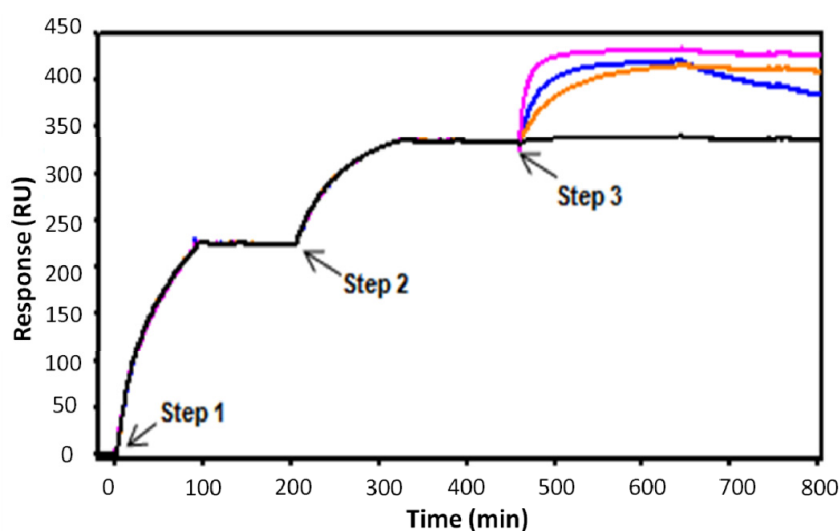


This study has provided a thorough dissection of binding kinetics for the five anti-ricin mAbs. We determined that mAbs 7G12 and 9C3 had the slowest dissociation rate while 11D7 had the fastest association rate. In a detection sensor format it is most practicable to utilize antibodies with slow dissociation for use as capture reagents, whilst non-competing mAbs with weaker affinities may then be employed as secondary reagents that bind and confirm the presence of captured ricin. Tran *et al.* [25] showed the potential of 7G12 mAb as a platform capture reagent for detection of ricin. The high affinity of this antibody for ricin allowed for the detection of ricin in both commercial preparations and environment samples using the Biacore X platform. In this study we have shown that 7G12 mAbs tight affinity for ricin is mainly driven by its slow dissociation rate thus making this mAb very-well suited as a capture reagent. Additionally, our work demonstrates the utility of four other mAbs in an SPR based ricin detection biosensor platforms. Thus, 14F11 mAb is unlikely to be suitable as a capture agent, owing to its fast dissociation kinetics, yet it may suffice as a secondary reagent as slower dissociation would be enhanced as a result of its bivalent nature and this avidity effect may drive

tighter binding. Nevertheless, given that 9C3 mAb binds the same epitope with greater affinity, it perhaps represents a preferable mAb for use as a capture or secondary detection reagent.

Recombinant antibody fragments such as Fabs, scFv and sdAbs are valuable alternatives to full length monoclonal antibodies for use in biosensor devices as they provide smaller, yet stable and highly specific reagents against the target antigen [23,27]. To further investigate the panel of six mAbs we have cloned variable heavy and light gene fragments and reformatted these as recombinant Fab fragments for expression in *E. coli*. Of these, only 8G2, 14F11 and 9C3 rFab were expressed at significant levels using standard expression conditions. More importantly, 9C3 and 14F11 rFabs bound ricin with near identical affinities as their parental mAbs. Considering the sequence similarity, we hypothesized that the difference in binding kinetics for these two rFabs could be attributed to the CDR3 region of the light chain. By combining the heavy chain of 14F11 rFab with the light chain of 9C3 rFab, we generated a chained-shuffled rFab (14F11H/9C3L) with a significantly higher binding affinity for ricin. Figure 7 illustrates SPR sandwich assays for detection of ricin where 7G12 mAb is used for ricin capture and recombinant Fabs are used as secondary (detection) reagents. Results demonstrate that the slowly dissociating chain-shuffled and 9C3 rFab constructs perform better in the sandwich assay than the faster dissociating 14F11 rFab.

Figure 7. SPR sandwich assay for detection of ricin using 7G12 mAb for capture and rFabs as secondary detecting reagents. Four different assays (sensorgrams) are overlaid in the diagram. Step 1: Injection & capture 7G12 mAb onto a CM5 chip surface containing rabbit anti-mouse IgG, Fc specific polyclonal antibody; Step 2: Injection and binding of ricin (at 100 nM) to captured 7G12 mAb; Step 3: Injection & binding of rFabs to captured ricin (all at 50 nM)—chain-shuffled construct (magenta), 14F11 (blue), 9C3 (orange) and 8G2 rFab (black, negative control showing no binding to captured ricin).



Ricin-toxicity inhibition assay showed the significantly improved binding efficacy of this chain-shuffled rFab construct. Based on our SPR measurements we concluded that the difference in the level on ricin-toxicity inhibition between the 14F11, 9C3 and chained-shuffled rFabs was predominantly due to differences in dissociation rates, with the chain-shuffled rFab having the slowest k_d and consequently displaying the best inhibition properties. Recently, although through more

sophisticated means, an increased affinity of a chimeric anti-ricin antibody C4C13 was achieved through structure based maturation [28]. Vance *et al.* [29] used a stepwise approach to engineer single-chain camelid V_H domains to enhance ricin toxin-neutralizing antibodies. Quite clearly, a slower dissociation parameter correlates with a more stable antibody-ricin complex and consequently a decreased probability of ricin toxicity [30].

3. Experimental

3.1. Ricin and Chemical Reagents

Ricin toxin, RTA and RTB were obtained from Sigma-Aldrich (NSW, Australia). The amount of ricin toxin maintained in the laboratory was less than 5 mg and therefore exempt from SSBA registration with the Australian government. Biacore T100 reagents were from GE-Healthcare (Uppsala, Sweden). ProteOn XPR36 biosensor reagents were from Bio-Rad (Hercules, CA, USA). Oligonucleotide primers (Table 3) were purchased from Geneworks (SA, Australia).

Table 3. Oligonucleotide primers.

Primer designation	Sequence (5'-3')
A1437	CAGGTCACTGTCACTGGCTCAG
A1436	CTTCCACTTGACATTGATGTCTTTG
Poly-C anchor sense	ATCGATGAATTCCGGATCCCCCCCCCCCCCCCC
A1706	TGCAGAGACGGTGACCAGAGTCCCTTGGCCCCA
A1713	CAGCCGGCCATGGCTGAGGTCCAGCTGCAGCAG
9C3-K5'	GACGCCGATATCGATGACCCAAACTCCACT
9C3-K3'	TTTTATCTCGAGCTTGGTCCCCCGCCGAA
15C5-K5'	CAGGCCGATATCGTGATGACCCAAACTCCA
14F11-K3'	TTTCAGCTCGAGCTTGGTCCCAGCACCGAA

3.2. Cultivation of Hybridoma Cell Lines and Production of mAbs

Murine hybridoma cell lines producing antibody (all IgG1/κ) directed against ricin were adapted to defined hybridoma serum-free medium (Invitrogen, CA, USA) containing ciprofloxacin and grown at 37 °C under a 10% CO₂ humidified atmosphere. On the final day of incubation the supernatant was collected for purification.

3.3. Purification of mAbs

Monoclonal antibodies in serum-free hybridoma supernatants were passed through a 0.22 μm filter and applied to a Prosep-vA column (Millipore, MA, USA). After washing with phosphate-buffered saline (1 × PBS), bound mAb was eluted with 0.2 M glycine pH 2.0, neutralized with 1 M Tris, pH 8.0 and dialysed against 1 × PBS containing 0.02% (w/v) sodium azide. Purity of the mAb preparations was determined by SDS-PAGE using a 10% NuPAGE[®] Novex Bis-Tris gel (Invitrogen) and by size exclusion chromatography using either a Superdex 200 HR 10/30 column (GE Healthcare) at a flow rate of 0.5 mL/min or a BioSep-S2000 column (Phenomenex, CA, USA) at a flow rate of 1 mL/min.

Columns were calibrated with Bio-Rad Gel Filtration Standard proteins. The concentration of purified mAbs was determined by absorbance spectroscopy [31].

3.4. Cloning and Sequencing of Antibody Variable Regions

Anti-ricin hybridoma cell lines [24] were used as sources for the preparation of V_H and V_L cDNA gene fragments. The method of Gilliland *et al.* [32] was adapted for the extraction of RNA and subsequent cDNA synthesis. Total cellular RNA was extracted from 5×10^6 hybridoma cells using TRIzol reagent (Invitrogen) and poly-A⁺ RNA was isolated from total cellular RNA employing the Oligotex mRNA mini kit (Qiagen, Vic., Australia). Single-stranded (ss) cDNA was produced by reverse-transcription of RNA using the Omniscript reverse transcriptase kit (Qiagen). Reactions contained 500 ng of poly-A⁺ RNA and 10 pmol of isotype-specific anti-sense oligonucleotide primer (A1437 for CH1- γ 1 and A1436 for CL- κ cDNA). A poly-G tail was appended to the 3'-end of ss-cDNA using terminal transferase (NEB, MA, USA). Double-stranded cDNA was generated by PCR using *Vent* polymerase (NEB) with the poly-C anchor and C_H- γ 1 or C_L- κ specific primers. PCR cycling consisted: 40 cycles of 60-s at 94 °C, 30-s at 55 °C and 30-s at 72 °C. PCR products were resolved by agarose gel electrophoresis and subcloned into PCR-script Amp vector (Stratagene, CA, USA). The V_H and V_L genes were sequenced and aligned using Clone Manager 9 Professional Edition. The GenBank accession numbers for anti-ricin mAb V_H and V_L sequences are: 7G12-**FN686796** (V_H)/**FN686797** (V_L), 8G2-**FN686798** (V_H)/**FN686799** (V_L), 9C3-**FN686800** (V_H)/**FN686801** (V_L), 11D7-**FN686802** (V_H)/**FN686803** (V_L), 14F11-**FN686804** (V_H)/**FN686805** (V_L) and 15C5-**FN686806** (V_H)/**FN686807** (V_L).

3.5. Plasmid Vector Construction, Expression and Purification of Anti-Ricin rFabs

The genes encoding recombinant anti-ricin Fabs were cloned into the pGC plasmid [33] as shown in Figure 4. Briefly, a rFab expression cassette (synthesized by Genscript, NJ, USA) containing human CH1 (γ 1) and CL (κ) gene sequence was digested with *Nco*I and *Not*I restriction enzymes and cloned into the corresponding sites in pGC to generate pGC/[huchcl]. 9C3 and 14F11 V_H and V_L gene sequences were amplified by PCR using primers A1706/A1713 for V_H and 9C3-K5'/9C3-K3' and 15C5-K5'/14F11-K3' for V_L. The resulting PCR products encoding V_H and V_L gene sequences were digested with appropriate restriction enzymes (*Nco*I and *Bst*EII for V_H and *Eco*RV/*Xho*I for V_L) and cloned into the corresponding sites in pGC/[huchcl] to create pGC/anti-ricin rFab expression vectors (Figure 4).

Recombinant Fab clones were expressed as described in Dolezal *et al.* [34] and the resulting proteins purified from periplasmic extracts using a purification procedure described in Robert *et al.* [35]. Briefly, rFab proteins were affinity-purified via the construct's hexaHis tag using a 1-ml HisTrap FF cartridge (GE Healthcare) and then further purified on a cation exchange chromatography column (1-mL HiTrap SP, GE Healthcare). The eluted protein was concentrated to >1 mg/mL and applied to a Superdex 200 HR 10/30 size exclusion column (GE Healthcare) pre-equilibrated in 1 \times PBS buffer. Collected Fab proteins were concentrated to ~0.4–1 mg/mL using Pall Microsep centrifugal devices (Cheltenham Vic, Australia) and stored in 500 μ L aliquots at –20 °C. The concentration of purified rFab fragments was determined by absorbance spectroscopy [31].

3.6. Epitope Binning Experiments

Epitope binning analyses of anti-ricin mAbs was performed using a ProteOn sandwich assay described previously [36]. The ProteOn XPR36 array biosensor uses surface plasmon resonance (SPR) to monitor the interaction between immobilized ligands and injected analytes in real-time [37]. Six mAbs previously shown to bind ricin (8G2, 14F11, 9C3, 11D7, 15C5 and 7G12) were immobilized onto six channels of a GLM chip in the vertical (ligand) direction by employing a three step process. Briefly, six flow cells were activated in parallel for 5 min with a freshly mixed solution of 10 mM EDC in 2.5 mM sulfo-NHS. Antibodies were then coupled to the chip at a concentration of 100 µg/mL in 10 mM sodium acetate, pH 4.5 for 5 min. Excess reactive succinimide ester groups were blocked with 1 M ethanolamine pH 8.5 for 5 min. Final mean levels of immobilized mAbs ranged from 8705 to 3505 RU. Ricin was injected at 50 nM over the immobilized mAbs, also in the vertical (ligand) direction. Following rotation of the fluidics, mAbs (100 nM) were injected in separate channels in the horizontal (analyte) direction and binding to ricin was monitored over time.

3.7. Kinetic Binding Analysis of mAbs

Biacore T100 SPR instrument [38] was utilized to measure the binding interactions of mAbs with ricin. Immobilization and binding experiments were performed in HBS-EP+ running buffer (10 mM HEPES pH 7.5, 150 mM NaCl, 3 mM EDTA, 0.05% (v/v) Tween 20) at 25 °C. Approximately 2000 RU (1 RU = 1 pg of protein/mm²) of rabbit anti-mouse IgG, Fc specific polyclonal antibody (RAM Fc, GE Healthcare) was coupled to a CM5 chip using amine coupling chemistry as described by the supplier (GE Healthcare). Approximately 180 RU and 300 RU of RAM Fc was captured for RT and RTA/RTB kinetic analyses respectively with a contact time of 180-s and flow rate of 5 µL/min. Ricin concentrations (diluted two-fold from 50 nM to 1.56 nM) or RTA/RTB (100 nM to 2 nM) were each injected over the captured IgG at a flow rate of 30 µL/min and contact time of 240-s (RT) or 300-s (RTA and RTB) and a dissociation time of 300-s. The sensor surface was regenerated between each binding reaction with 10 mM glycine-HCl pH 1.5 with a flow rate of 30 µL/min and a contact time of 60-s. Binding data were processed and analyzed using Biacore T100 evaluation software and fit globally to a 1:1 binding model, $A + B = AB$, where A represents the injected analyte, B is the immobilized ligand, and AB is the analyte/ligand complex formed during the reaction.

3.8. Kinetic Binding Analysis of rFabs

Recombinant Fab binding analyses were performed with ricin immobilized on the CM5 chip surface. Ricin was manually immobilized to the chip using a standard amine coupling chemistry method as described by instrument manufacturer (GE Healthcare). The carboxymethyl surface of the CM5 chip was activated for 7 min at a flow rate of 10 µL/min using a 1:1 ratio of 0.4 M EDC and 0.1 M NHS. Ricin was diluted to 3.4 µg/mL in 10 mM sodium acetate pH 5.0 and gradually injected over the surface at a flow rate of 5 µL/min until 100 RU of RT was immobilized. Excess activated groups were blocked using a 7 min injection of 1 M ethanolamine, pH 8.5, at a flow rate of 10 µL/min. rFab at different concentrations were sequentially injected over immobilized ricin at a flow rate of 30 µL/min, contact time of 400-s and dissociation time of 900-s. The sensor surface was

regenerated between each binding event with 90 mM phosphoric acid with a flow rate of 30 $\mu\text{L}/\text{min}$ and contact time of 15-s. To calculate kinetic parameters of the ricin/rFab interactions, data from each experiment were processed and globally fit to a 1:1 binding model.

3.9. Antibody Neutralization of Ricin-Mediated Cytotoxicity

Small airway epithelial (SAE, Lonza Australia) human lung cells were grown in small airway growth medium (SAGM, Lonza) at 37 °C with 5% CO_2 . Cells were seeded in 96-well trays at a density of 1×10^4 per well and incubated overnight. Antibodies were diluted as required in SAGM containing 10 pM ricin and allowed to stand at room temperature for 15 min. Wells containing SAE cells were exposed to 100 μL of the antibody-ricin mixture in triplicate for 24 h at 37 °C. Cells were washed twice with $1 \times \text{PBS}$ and cell viability was measured using a neutral red (NR) assay in which cells were stained with 50 $\mu\text{g}/\text{mL}$ NR in SAGM at 37 °C for 3 h. Cells were subsequently washed twice with $1 \times \text{PBS}$, solubilized with 3 mM HCl in DMSO for 1 h and absorbance was measured at 540 nm. Means were normalized against cells treated with ricin only (no antibody) and expressed as a percentage of the negative control (cells only).

4. Conclusions

To develop sensitive and rapid ricin detection methods, high-affinity mAbs such as those discussed in this study are needed. Ideally, antibodies that bind to different epitopes on either the A or B subunit are required for efficient detection of ricin. Anderson *et al.* [22] reported on high affinity sdAbs against both RTA and RTB and their combined use in detection platforms that included sandwich ELISA and Luminex immunoassay. From the panel of six antibodies evaluated in this study, three epitopes, two from the B subunit and one for the A subunit, were identified. Furthermore, we have identified a best antibody combination for ricin detection, whereby the two highest affinity antibodies-7G12 (specific to subunit A) and the chain-shuffled 14F11/9C3 (subunit B) antibodies could be used either as primary capture and/or secondary detection reagents. Their slow dissociation kinetics, in particular, should prove useful not only in the detection of ricin but also, after appropriate reformatting, for prevention and/or treatment of ricin intoxication.

Acknowledgments

We thank Phillip Strike for N-terminal sequencing and Deborah Shapira for culturing of the hybridoma cell lines.

Authors Contributions

Conceived and designed the experiments: MC, MA, DP, SN and OD. Performed the experiments: MC, CD, RR, DC, LP-B, AR, MH and OD. Analysed the data: MC, DC, MH and OD. Wrote the paper: MC, CD, SN and OD.

Conflicts of Interest

The authors declare no conflict of interest.

References

1. Foxwell, B.M.; Detre, S.I.; Donovan, T.A.; Thorpe, P.E. The use of anti-ricin antibodies to protect mice intoxicated with ricin. *Toxicology* **1985**, *34*, 79–88.
2. Guo, J.W.; Shen, B.F.; Feng, J.N.; Sun, Y.X.; Yu, M.; Hu, M.R. A novel neutralizing monoclonal antibody against cell-binding polypeptide of ricin. *Hybridoma (Larchmt)* **2005**, *24*, 263–266.
3. Olsnes, S.; Pihl, A. Different biological properties of the two constituent peptide chains of ricin, a toxic protein inhibiting protein synthesis. *Biochemistry* **1973**, *12*, 3121–3126.
4. Baenziger, J.U.; Fiete, D. Structural determinants of ricinus communis agglutinin and toxin specificity for oligosaccharides. *J. Biol. Chem.* **1979**, *254*, 9795–9799.
5. Alami, M.; Taupiac, M.P.; Beaumelle, B. Ricin-binding proteins along the endocytic pathway: The major endosomal ricin-binding protein is endosome-specific. *Cell Biol. Int.* **1997**, *21*, 145–150.
6. Lord, J.M.; Deeks, E.; Marsden, C.J.; Moore, K.; Pateman, C.; Smith, D.C.; Spooner, R.A.; Watson, P.; Roberts, L.M. Retrograde transport of toxins across the endoplasmic reticulum membrane. *Biochem. Soc. Trans.* **2003**, *31*, 1260–1262.
7. Sandvig, K.; Ryd, M.; Garred, O.; Schweda, E.; Holm, P.K.; van Deurs, B. Retrograde transport from the golgi complex to the er of both shiga toxin and the nontoxic shiga b-fragment is regulated by butyric acid and camp. *J. Cell Biol.* **1994**, *126*, 53–64.
8. Mlsna, D.; Monzingo, A.F.; Katzin, B.J.; Ernst, S.; Robertus, J.D. Structure of recombinant ricin a chain at 2.3 a. *Protein Sci.* **1993**, *2*, 429–435.
9. Chen, X.Y.; Link, T.M.; Schramm, V.L. Ricin a-chain: Kinetics, mechanism, and rna stem-loop inhibitors. *Biochemistry* **1998**, *37*, 11605–11613.
10. Endo, Y.; Mitsui, K.; Motizuki, M.; Tsurugi, K. The mechanism of action of ricin and related toxic lectins on eukaryotic ribosomes. The site and the characteristics of the modification in 28 s ribosomal rna caused by the toxins. *J. Biol. Chem.* **1987**, *262*, 5908–5912.
11. Pincus, S.H.; Smallshaw, J.E.; Song, K.; Berry, J.; Vitetta, E.S. Passive and active vaccination strategies to prevent ricin poisoning. *Toxins (Basel)* **2011**, *3*, 1163–1184.
12. McGuinness, C.R.; Mantis, N.J. Characterization of a novel high-affinity monoclonal immunoglobulin g antibody against the ricin b subunit. *Infect. Immun.* **2006**, *74*, 3463–3470.
13. Reisler, R.B.; Smith, L.A. The need for continued development of ricin countermeasures. *Adv. Prev. Med.* **2012**, *2012*, 149737.
14. Smallshaw, J.E.; Vitetta, E.S. A lyophilized formulation of rivax, a recombinant ricin subunit vaccine, retains immunogenicity. *Vaccine* **2010**, *28*, 2428–2435.
15. Neal, L.M.; O'Hara, J.; Brey, R.N.; Mantis, N.J. A monoclonal immunoglobulin g antibody directed against an immunodominant linear epitope on the ricin a chain confers systemic and mucosal immunity to ricin. *Infect. Immun.* **2010**, *78*, 552–561.
16. Prigent, J.; Panigai, L.; Lamourette, P.; Sauvaire, D.; Devilliers, K.; Plaisance, M.; Volland, H.; Creminon, C.; Simon, S. Neutralising antibodies against ricin toxin. *PLoS One* **2011**, *6*, e20166.
17. Hu, W.G.; Yin, J.; Chau, D.; Negrych, L.M.; Cherwonogrodzky, J.W. Humanization and characterization of an anti-ricin neutralization monoclonal antibody. *PLoS One* **2012**, *7*, e45595.
18. Sheridan, C. Fresh from the biologic pipeline-2009. *Nat. Biotechnol.* **2010**, *28*, 307–310.

19. Kim, S.J.; Park, Y.; Hong, H.J. Antibody engineering for the development of therapeutic antibodies. *Mol. Cells* **2005**, *20*, 17–29.
20. Pelat, T.; Hust, M.; Hale, M.; Lefranc, M.P.; Dübel, S.; Thullier, P. Isolation of a human-like antibody fragment (scfv) that neutralizes ricin biological activity. *BMC Biotechnol.* **2009**, *9*, 60.
21. Anderson, G.P.; Liu, J.L.; Hale, M.L.; Bernstein, R.D.; Moore, M.; Swain, M.D.; Goldman, E.R. Development of antiricin single domain antibodies toward detection and therapeutic reagents. *Anal. Chem.* **2008**, *80*, 9604–9611.
22. Anderson, G.P.; Bernstein, R.D.; Swain, M.D.; Zabetakis, D.; Goldman, E.R. Binding kinetics of antiricin single domain antibodies and improved detection using a b chain specific binder. *Anal. Chem.* **2010**, *82*, 7202–7207.
23. Walper, S.A.; Brozozog Lee, P.A.; Goldman, E.R.; Anderson, G.P. Comparison of single domain antibody immobilization strategies evaluated by surface plasmon resonance. *J. Immunol. Methods* **2013**, *388*, 68–77.
24. Dertzbaugh, M.T.; Rossi, C.A.; Paddle, B.M.; Hale, M.; Poretski, M.; Alderton, M.R. Monoclonal antibodies to ricin: *In vitro* inhibition of toxicity and utility as diagnostic reagents. *Hybridoma (Larchmt)* **2005**, *24*, 236–243.
25. Tran, H.; Leong, C.; Loke, W.K.; Dogovski, C.; Liu, C.Q. Surface plasmon resonance detection of ricin and horticultural ricin variants in environmental samples. *Toxicon* **2008**, *52*, 582–588.
26. Butler, J.E.; Navarro, P.; Sun, J. Adsorption-induced antigenic changes and their significance in elisa and immunological disorders. *Immunol. Invest.* **1997**, *26*, 39–54.
27. Anderson, G.P.; Glaven, R.H.; Algar, W.R.; Susumu, K.; Stewart, M.H.; Medintz, I.L.; Goldman, E.R. Single domain antibody-quantum dot conjugates for ricin detection by both fluoroimmunoassay and surface plasmon resonance. *Anal. Chim. Acta* **2013**, *786*, 132–138.
28. Luo, L.; Luo, Q.; Guo, L.; Lv, M.; Lin, Z.; Geng, J.; Li, X.; Li, Y.; Shen, B.; Qiao, C.; *et al.* Structure-based affinity maturation of a chimeric anti-ricin antibody c4c13. *J. Biomol. Struct. Dyn.* **2014**, in press.
29. Vance, D.J.; Tremblay, J.M.; Mantis, N.J.; Shoemaker, C.B. Stepwise engineering of heterodimeric single domain camelid vhh antibodies that passively protect mice from ricin toxin. *J. Biol. Chem.* **2013**, *288*, 36538–36547.
30. Song, K.; Mize, R.R.; Marrero, L.; Corti, M.; Kirk, J.M.; Pincus, S.H. Antibody to ricin a chain hinders intracellular routing of toxin and protects cells even after toxin has been internalized. *PLoS One* **2013**, *8*, e62417.
31. Gill, S.C.; von Hippel, P.H. Calculation of protein extinction coefficients from amino acid sequence data. *Anal. Biochem.* **1989**, *182*, 319–326.
32. Gilliland, L.K.; Norris, N.A.; Marquardt, H.; Tsu, T.T.; Hayden, M.S.; Neubauer, M.G.; Yelton, D.E.; Mittler, R.S.; Ledbetter, J.A. Rapid and reliable cloning of antibody variable regions and generation of recombinant single chain antibody fragments. *Tissue Antigens* **1996**, *47*, 1–20.
33. Coia, G.; Ayres, A.; Lilley, G.G.; Hudson, P.J.; Irving, R.A. Use of mutator cells as a means for increasing production levels of a recombinant antibody directed against hepatitis b. *Gene* **1997**, *201*, 203–209.

34. Dolezal, O.; Pearce, L.A.; Lawrence, L.J.; McCoy, A.J.; Hudson, P.J.; Kortt, A.A. Scfv multimers of the anti-neuraminidase antibody nc10: Shortening of the linker in single-chain fv fragment assembled in v(l) to v(h) orientation drives the formation of dimers, trimers, tetramers and higher molecular mass multimers. *Protein Eng.* **2000**, *13*, 565–574.
35. Robert, R.; Streltsov, V.A.; Newman, J.; Pearce, L.A.; Wark, K.L.; Dolezal, O. Germline humanization of a murine abeta antibody and crystal structure of the humanized recombinant fab fragment. *Protein Sci.* **2010**, *19*, 299–308.
36. Abdiche, Y.; Malashock, D.; Pinkerton, A.; Pons, J. Determining kinetics and affinities of protein interactions using a parallel real-time label-free biosensor, the octet. *Anal. Biochem.* **2008**, *377*, 209–217.
37. Bravman, T.; Bronner, V.; Lavie, K.; Notcovich, A.; Papalia, G.A.; Myszka, D.G. Exploring “one-shot” kinetics and small molecule analysis using the proteon xpr36 array biosensor. *Anal. Biochem.* **2006**, *358*, 281–288.
38. Papalia, G.A.; Baer, M.; Luehrsen, K.; Nordin, H.; Flynn, P.; Myszka, D.G. High-resolution characterization of antibody fragment/antigen interactions using biacore t100. *Anal. Biochem.* **2006**, *359*, 112–119.

© 2014 by the authors; licensee MDPI, Basel, Switzerland. This article is an open access article distributed under the terms and conditions of the Creative Commons Attribution license (<http://creativecommons.org/licenses/by/3.0/>).